した（**図2**）。次に，過剰量を静脈内投与することで，非晶質ナノシリカの妊娠マウスに対するハザード同定を試みた。その結果，nSP70-N，および nSP70-C 投与群において異常が認められなかった一方で，nSP70 投与群でのみ，胎仔吸収率の増加とともに，胎仔体重がコントロール群よりも 10% 以上減少するなど，胎仔発育不全を誘発していることが明らかとなった。なお，これら粒子の胎盤への集積や胎仔への移行，および胎仔への影響は，nSP300，および mSP1000 では認められていない。このことから，多くの非晶質ナノシリカ素材が，生殖発生毒性学的視点からも安全であるものの，一部の素材については注意を払う必要があることが示された。以上の検討で見出された nSP70 のハザードは，過剰量における検討ではあるものの，従来型非晶質シリカである nSP300，mSP1000 では認められなかったものであり，一部の非晶質ナノシリカが従来型の非晶質シリカとは異なる生体影響を誘発する可能性を示している。一方で nSP70-N，nSP70-C は，過剰量を静脈内に投与するという実験系にもかかわらず，目立ったハザードは認められなかったことから，これらはきわめて安全性の高い素材であると考えられる。また，これらの知見は逆に，ごく一部の安全性に懸念のあるものに関しても，適切な表面修飾を施すことにより，安全性を担保できる可能性を示している。ナノマテリアルの中にも安全性が高いものとそうでないものがあることはよく知られているが，今後，安全なナノマテリアルを創製するための方法論といったナノ安全科学研究に関する情報をより多く収集することが，ナノマテリアルの安全性評価研究の最重要課題の1つであると考えている。

4. おわりに――ナノ DDS 医薬品の将来像

本総説では，ナノ DDS への適用の現状とともに，最も急がれる安全性確保に関する検討を中心に紹介した。最近では，カーボンナノ素材や非晶質ナノシリカに加え，抗酸化・抗菌活性などを有した白金や

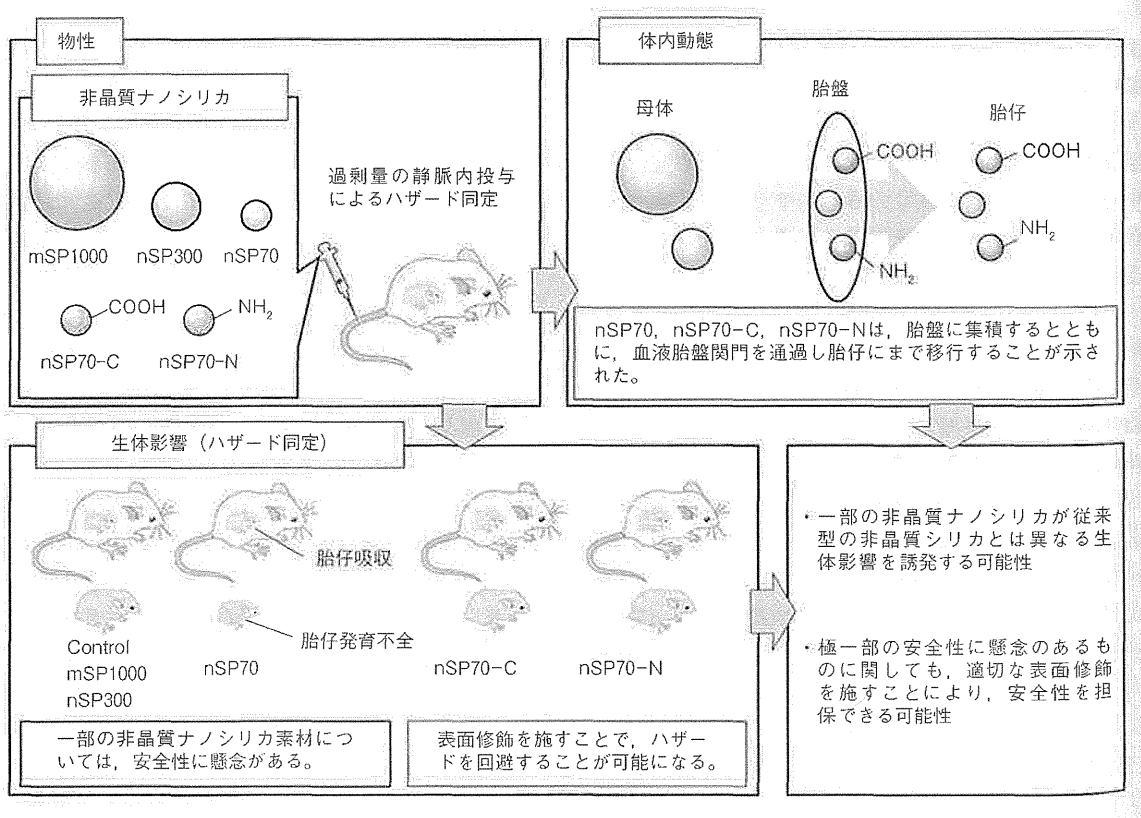

図2　生殖発生毒性学的視点からの非晶質ナノシリカの安全性評価

銀などに関して，タンパク質と同等のサブナノサイズ領域（10 nm 以下）の素材（サブナノ素材）の開発・実用化も進んでいる。しかし現状では，地球規模でナノマテリアルやサブナノ素材の安全性に警鐘が鳴らされ，OECD を含め，欧米では規制が進んでいるものの，わが国を鑑みると，薬事法・薬局方（医薬品・化粧品・医薬部外品など）をはじめとする各種法律を見ても，ナノマテリアルやサブナノ素材に言及した規制はない。さらに，これら各種法律においては，ナノマテリアルやサブナノ素材を構成する化学物質の構造式（物質名）のみで規制されているため，従前のサブミクロンサイズ（100 nm）以上の素材で安全性が確認されたものや，経験的に安全と考えられるものであれば，ナノ化・サブナノ化されたものでも自由に利用できてしまうことになる。すなわち，①ナノ化・サブナノ化によって，安全性を運命づける『動態特性や効能・効果』が，同一素材であっても，従前のサブミクロンサイズ以上の素材や分子状素材と大きく変動し得ること，②物性などによっても，ナノマテリアルやサブナノ素材に特有の性能が変動し得ること，が理解されつつあるにもかかわらず，品質管理・保障の規制・ガイドライン策定には程遠いのが現状である。したがって，今後は，物性・品質と，動態情報や安全性情報の連関解析を定量的に実施する必要があると考えられる。このように，Nano-Safety Science の視点から，ナノマテリアルの安全性情報を収集したうえで，Nano-Safety Design の視点から，安全性の高いものは実用化を推進し，安全性の低いものは表面性状制御をはじめとした適切な方策を講じて安全性を高めていくことで，ヒト健康の確保と同時に，われわれがナノテクノロジーの恩恵を享受しつつナノ産業界の発展も達成できるものと考えている。今後，ナノ開発研究とナノ安全科学研究が強固に連携し，両輪となってともに歩むことで，Sustainable Nanotechnology（いわゆる，持続可能なナノテクノロジー）に資する，地球・環境・ヒトに優しい（安全な）ナノマテリアルの創製，ひいてはナノ医薬品の開発が飛躍的に進歩することを楽しみに，筆者らも一緒にチャレンジしたい。

【引用・参考文献】

1) K. Ajima, et al.：*Mol. Pharm.*, **2**, 475 (2005).
2) Y. Tabata, et al.：*Jpn. J. Cancer Res.*, **88**, 1108 (1997).
3) C. A. Poland, et al.：*Nat. Nanotechnol.*, **3**, 423 (2008).
4) G. Oberdörster, et al.：*J. Nanosci. Nanotechnol.*, **9**, 4996 (2009).
5) H. Nabeshi, et al.：*Part. Fibre Toxicol.*, **8**, 1 (2011).
6) T. Yoshida, et al.：*Nanoscale Res. Lett.*, **6**, 195 (2011).
7) K. Yamashita, et al.：*Inflammation*, **33**, 276 (2010).
8) H. Nabeshi, et al.：*Biomaterials*, **32**, 2713 (2011).
9) K. Yamashita, et al.：*Nat. Nanotechnol.*, **6**, 321 (2011).

〈東阪　和馬／堤　康央〉

Yoshida et al. Particle and Fibre Toxicology 2013, 10:41
http://www.particleandfibretoxicology.com/content/10/1/41

PARTICLE AND FIBRE TOXICOLOGY

RESEARCH Open Access

Intranasal exposure to amorphous nanosilica particles could activate intrinsic coagulation cascade and platelets in mice

Tokuyuki Yoshida[1], Yasuo Yoshioka[1*], Saeko Tochigi[1], Toshiro Hirai[1], Miyuki Uji[1], Ko-ichi Ichihashi[1], Kazuya Nagano[2], Yasuhiro Abe[3], Haruhiko Kamada[2,4], Shin-ichi Tsunoda[2,4], Hiromi Nabeshi[5], Kazuma Higashisaka[1], Tomoaki Yoshikawa[1] and Yasuo Tsutsumi[1,2,4*]

Abstract

Background: Nanomaterials with particle sizes <100 nm have been already applied in various applications such as cosmetics, medicines, and foods. Therefore, ensuring the safety of nanomaterials is becoming increasingly important. Here we examined the localization and biological responses of intranasally administered amorphous nanosilica particles in mice, focusing on the coagulation system.

Methods: We used nanosilica particles with diameters of 30, 70, or 100 nm (nSP30, nSP70, or nSP100 respectively), and conventional microscale silica particles with diameters of 300 or 1000 nm (mSP300 or mSP1000, respectively). BALB/c mice were intranasally exposed to nSP30, nSP70, nSP100, mSP300, or mSP1000 at concentrations of 500 μg/mouse for 7 days. After 24 hours of last administration, we performed the *in vivo* transmission electron microscopy analysis, hematological examination and coagulation tests.

Results: *In vivo* transmission electron microscopy analysis showed that nanosilica particles with a diameter <100 nm were absorbed through the nasal cavity and were distributed into liver and brain. Hematological examination and coagulation tests showed that platelet counts decreased and that the activated partial thromboplastin time was prolonged in nSP30 or nSP70-treated groups of mice, indicating that nanosilica particles might have activated a coagulation cascade. In addition, in *in vitro* activation tests of human plasma, nanosilica particles had greater potential than did conventional microscale silica particles to activate coagulation factor XII. In nanosilica-particle-treated groups, the levels of soluble CD40 ligand, and von Willebrand factor which are involved in stimulating platelets tended to slightly increase with decreasing particle size.

Conclusions: These results suggest that intranasally administered nanosilica particles with diameters of 30 and 70 nm could induce abnormal activation of the coagulation system through the activation of an intrinsic coagulation cascade. This study provides information to advance the development of safe and effective nanosilica particles.

Keywords: Nanomaterials, Silica, Platelet, Coagulation

* Correspondence: yasuo@phs.osaka-u.ac.jp; ytsutsumi@phs.osaka-u.ac.jp
[1]Laboratory of Toxicology and Safety Science, Graduate School of Pharmaceutical Sciences, Osaka University, 1-6 Yamadaoka, Suita, Osaka 565-0871, Japan
[2]Laboratory of Biopharmaceutical Research, National Institute of Biomedical Innovation, 7-6-8 Saitoasagi, Ibaraki, Osaka 567-0085, Japan
Full list of author information is available at the end of the article

Background

Over the past decade, the field of nanotechnology has developed remarkably, and nanomaterials (NMs), which are defined as objects with a diameter less than 100 nm, have been created for various applications. For example, NMs have already been included in many consumer products, such as cosmetics, food, and medicine, to improve their stability and efficacy [1-3]. In particular, amorphous nanosilica particles are one of the most widely applied NMs and are used in cosmetics such as foundation and sunblock, in food additives, and as diluents for medicine [2,4]. As the number of commercial NMs increases, so do opportunities for human exposure to NMs, leading to increasing concern about the safety of NMs [5].

Concerns about the potential health risks of NMs have caused international organizations, such as the World Health Organization and the Organization for Economic Co-operation and Development, to call for an urgent and detailed evaluation of NMs' safety. To create effective and safer NMs, information about the biodistribution and biological effects of NMs must be acquired. Recent studies have reported that NMs may have unpredicted biological effects that conventional-sized materials do not possess [6,7]. For example, like crocidolite asbestos, carbon nanotubes induce mesothelioma-like lesions in mice [8]. Other reports have shown that exposure to titanium dioxide particles induces inflammatory responses and lung injury in mice [9,10]. In our previous study, we revealed that nanosilica particles could penetrate the skin and enter various tissues [11] and that nanosilica particles can cause pregnancy complications [12], immune-modulating effects [13,14], and consumptive coagulopathy after being absorbed into the whole body of mice [15]. In addition, we showed that nanosilica particles-mediated pregnancy complications and inflammation could be avoided by surface modification of the nanosilica particles with amino or carboxyl groups [12,16], suggesting that modification of the surface of nanosilica particles with amino or carboxyl groups may be effective for the creation of safer nanosilica particles. However, only a few studies have assessed the effects of nanosilica particles by realistic exposure pathways, such as oral or intranasal pathways. In particular, because nanosilica particles are used in the spray products, and inhalation opportunities of nanosilica particles in our life are increasing, such examination of biodistribution and biological responses following nasal exposure routes is urgently needed to advance the use of nanosilica particles in various applications.

Here, we have investigated the *in vivo* localization and biological effects of various sizes of nanosilica particles following intranasal administration in mice. In addition, we examined whether nanosilica particles could influence the coagulation system of mice. We expect that our results will contribute to the creation of safer NMs.

Results

Physicochemical examinations of silica particles

In this study, to assess the influence of the size of silica particles on *in vivo* localization or biological effects, we used nanosilica particles with diameters of 30, 70, or 100 nm (nSP30, nSP70, or nSP100, respectively), and conventional microscale silica particles with diameters of 300 or 1000 nm (mSP300 or mSP1000, respectively). In a previous study, we confirmed that the mean secondary particle diameters of each of these types of silica particles are 39, 76, 106, 264, and 1136 nm (for nSP30, nSP70, nSP100, mSP300, and mSP1000, respectively) by dynamic laser scattering analysis [11,12,14], and all the particles were confirmed to be well-dispersed smooth-surfaced spheres by transmission electron microscopy. These results indicate that the silica particles used in this study would remain stable and well-dispersed in solution, without aggregating.

In vivo localization of silica particles

First, we qualitatively examined the *in vivo* localization of silica particles after intranasal administration (Figure 1). BALB/c mice were intranasally exposed to nSP30, nSP70, nSP100, mSP300, or mSP1000 at concentrations of 500 μg/mouse for 7 days. Transmission electron microscopy analysis revealed that mSP1000 were located in mucosal epithelial cells of the nasal cavity (Figure 1a), and mSP300 and mSP1000 were located in type II alveolar epithelial cells of the lung (Figure 1b,e), although they were not detected in the liver (Figure 1c,f). On the other hand, nSP30, nSP70, and nSP100 were located not only in the nasal cavity (Figure 1g,j,m,p,s,v) and lung (Figure 1h,k,n,q, t,w) but also in hepatocytes in the liver (Figure 1i,l,o,r,u,x). These results suggested that nanosilica particles were absorbed through the nasal cavity and distributed into some tissues in the body. Therefore, to thoroughly evaluate the safety of these NMs, the biological effects of the intranasally administered silica particles might need to be evaluated for all tissues in the mouse body.

Biological effects induced by silica particles in tissue

To evaluate the effects of silica particles on the tissue in which they were present after intranasal administration, we observed the nasal cavity, brain, and liver of each mouse by hematoxylin–eosin staining (Figure 2). For all the groups of mice, although very slight inflammatory cell aggregation was observed in the nasal cavity, brain, and liver, these pathological findings were within normal ranges (Figure 2 and Table 1). Next, we measured the liver damage markers alanine aminotransferase (ALT) and albumin (ALB), as well as kidney damage marker blood urea nitrogen (BUN), in the tissues (Figure 3). Although the level of ALT in plasma increased slightly in nanosilica-particle-treated groups compared to the control group,

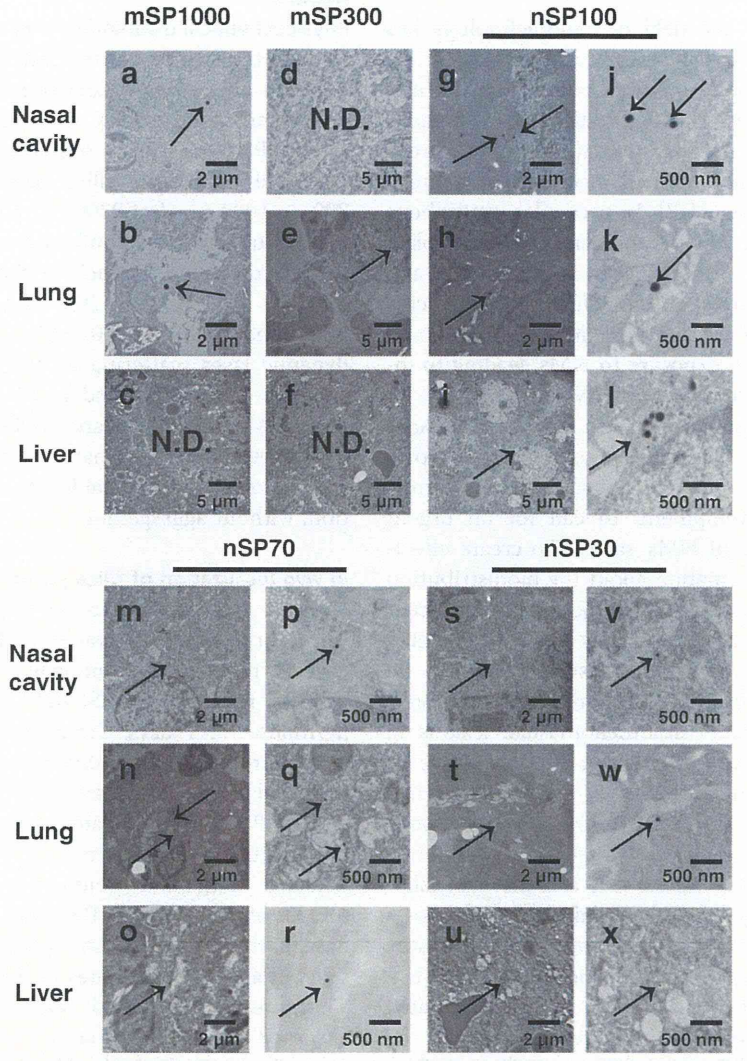

Figure 1 Biodistribution of silica particles. BALB/c mice were intranasally exposed to nSP30, nSP70, mSP300, nSP100, or mSP1000 at a concentration of 500 μg/mouse for 7 days. Twenty-four hours after the final administration, the nasal cavity **(a,d,g,j,m,p,s,v)**, lung **(b,e,h,k,n,q,t,w)**, and liver **(c,f,i,l,o,r,u,x)** were evaluated by transmission electron microscopy. Arrows point to silica particles. N.D.: not detected.

the change in the ALT value was within a normal, healthy range (<43 U/L) among all the groups (Figure 3a). BUN and ALB levels did not change significantly for any of the groups (Figure 3b,c). These results suggest that the intranasally administered nanosilica particles did not induce abnormal changes in some tissues.

Next, we performed hematological examination. As the size of the nanosilica particles decreased, so did the platelet counts in the silica-particle-treated groups, although the counts of other blood components (white blood cells, lymphocytes, and monocytes) remained unchanged in all groups (Figure 4a–d). The decrease in platelets was confirmed to occur in a dose-dependent manner in the nSP70- and nSP30-treated groups (Figure 4e,f). The platelet counts for nSP70 at concentrations below 250 μg/mouse and for nSP30 at concentrations below 62.5 μg/mouse were equal to those of the control group (Figure 4e,f). Thus, these findings suggest that intranasally administered nanosilica particles may decrease platelet counts.

Activation of coagulation system induced by silica particles

Previously, we revealed that a drastic decrease in platelets after systemic exposure to nSP70 could result from consumptive coagulopathy [15]. Therefore, we speculated that intranasally administered nanosilica particles might also induce a coagulation cascade. To evaluate the

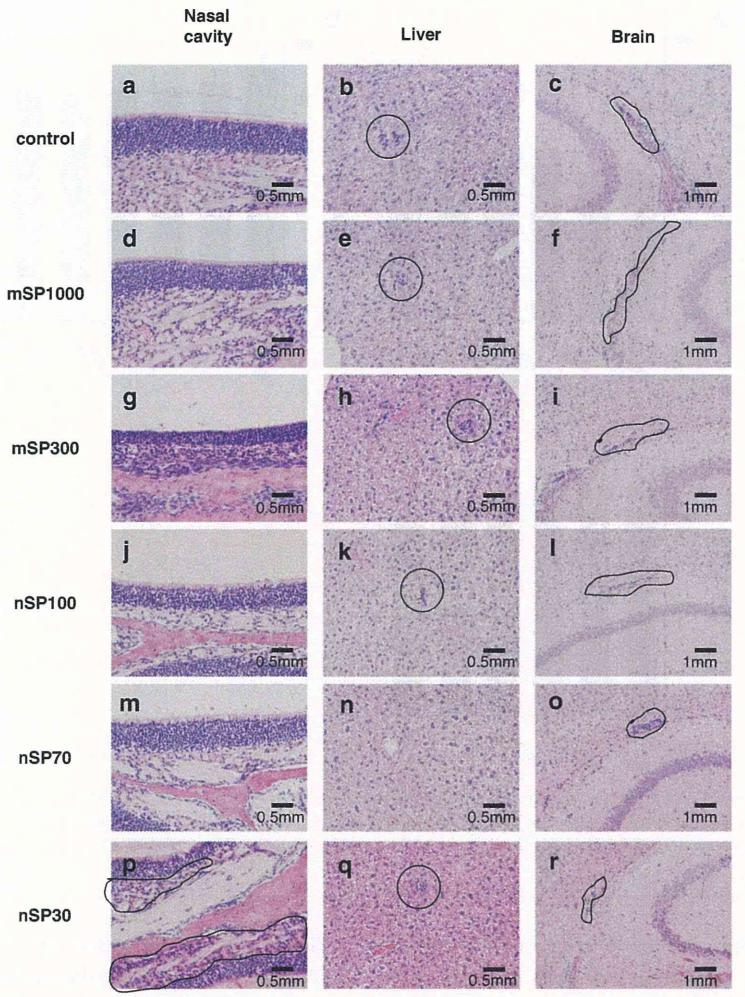

Figure 2 Histopathological analysis. BALB/c mice were intranasally exposed to nSP30, nSP70, mSP300, nSP100, or mSP1000 at a concentration of 500 μg/mouse for 7 days. Twenty-four hours after the final administration, nasal cavity **(a,d,g,j,m,p)**, liver **(b,e,h,k,n,q)** and brain **(c,f,i,l,o,r)** tissue samples were stained with hematoxylin–eosin. In images, solid line delineates cell aggregation. The histopathological grades of these samples are summarized in Table 1.

Table 1 Histopathological grades of nasal cavity, brain, and liver tissue samples collected from three different BALB/c mice exposed to nSP30, nSP70, mSP300, nSP100, or mSP1000 via intranasal administration

Findings	Control	mSP1000	mSP300	nSP100	nSP70	nSP30
Nasal cavity						
Cell aggregation	0 0 0	0 0 0	0 0 0	0 0 0	0 0 0	1 1 1
Brain						
Microglial aggregation	1 1 0	1 1 0	1 2 1	1 0 0	2 1 0	1 1 1
Liver						
Cell aggregation	1 2 0	1 2 1	1 1 0	1 1 1	0 0 0	0 1 1
Rarefaction	3 3 2	3 3 2	3 3 3	3 3 3	3 2 2	3 3 2

Grade; 0: none, 1: very slight, 2: mild, 3: moderate, 4: advanced.

effect of nanosilica particles on the coagulation cascade, we measured the bleeding time of whole blood from each silica-particle-treated mouse by Duke's method (Figure 5a). Bleeding time was prolonged in the nSP30- and nSP70-treated groups compared to the control group, although the bleeding times of the nSP100-, mSP300-, and mSP1000-treated groups did not change (Figure 5a). These results suggest that intranasal exposure to nanosilica particles could induce abnormal activation of the coagulation system and thus leads to the consumptive coagulopathy.

Next, we examined the mechanism of abnormal activation of the coagulation system induced by nanosilica particles after intranasal administration. The blood coagulation system can be initiated by two pathways: an extrinsic cascade pathway, which is triggered by the release of tissue factor (TF) from the site of injury, and an

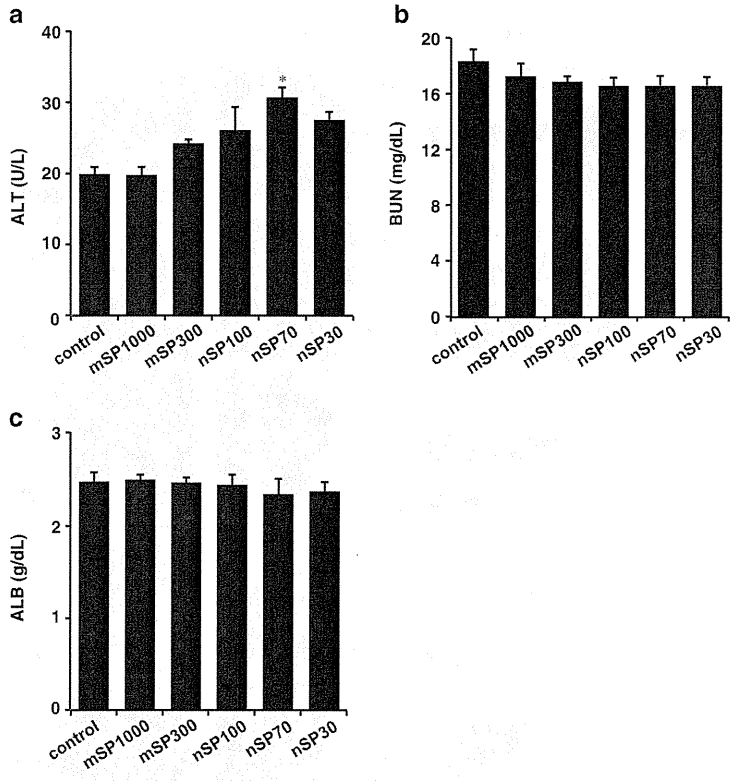

Figure 3 Biochemical analysis. BALB/c mice were intranasally exposed to nSP30, nSP70, mSP300, nSP100, or mSP1000 at a concentration of 500 μg/mouse for 7 days. Twenty-four hours after the final administration, plasma was collected. **(a)** alanine aminotransferase (ALT), **(b)** blood urea nitrogen (BUN), and **(c)** albumin (ALB) were analyzed. Results are expressed as mean ± S.E. (n = 4–5). *Represents significant difference from the control ($p < 0.05$).

intrinsic cascade pathway, which is triggered by activation of coagulant factor contacted with a negatively charged substance or accumulation of activated platelets to the collagen layer under the vascular endothelium [17]. We examined which cascade pathway was involved in the abnormal activation of the coagulation cascade by nanosilica particles after intranasal administration. The levels of prothrombin time (PT) (Figure 5b) and TF (Figure 5c), parameters for the activation of an extrinsic coagulation pathway, and activated partial thromboplastin time (APTT) (Figure 5d), a parameter for the activation of an intrinsic coagulation pathway, were measured in the plasma of each silica-particle-treated mouse. The levels of PT and TF did not vary compared to those observed for the control group (Figure 5b,c). In contrast, APTT in plasma from the nSP30- or nSP70-treated group was remarkably prolonged compared to that of the control group, although no change in APTT was observed for the nSP100-, mSP300-, or mSP1000-treated group (Figure 5d). These results suggest that the activation of an intrinsic cascade pathway induced by nanosilica particles could result in abnormal activation of the coagulation system.

Generally, the activation of an intrinsic cascade pathway is initiated by coagulation factor XII when it comes into contact with hydrophilic activating particles (such as fully water-wettable glass) [18]. Platelet activation is also involved in the activation of intrinsic cascade pathways [19]. We thus performed *in vitro* activation tests of coagulation factor XII using human plasma to confirm the presence of an intrinsic cascade pathway. One of our overall research goals is to contribute to the development of NMs that will be effective as well as safe for human exposure. To conduct a preliminary evaluation of the effects of nanosilica particles on humans, we used human plasma in the experiment, rather than mouse plasma. The *in vitro* activation tests showed that all sizes of the silica particles had the potential to activate coagulation factor XII, with activation apparently increasing as the size of the particles decreased (Figure 6a). In addition, to evaluate the activation of platelets, we measured the level of soluble CD40 ligand (sCD40L) and von Willebrand factor (vWF), which are involved in stimulating platelets [20,21], in the plasma of each silica-particle-treated mouse. In nanosilica-particle-treated groups, the levels of sCD40L and vWF tended to slightly

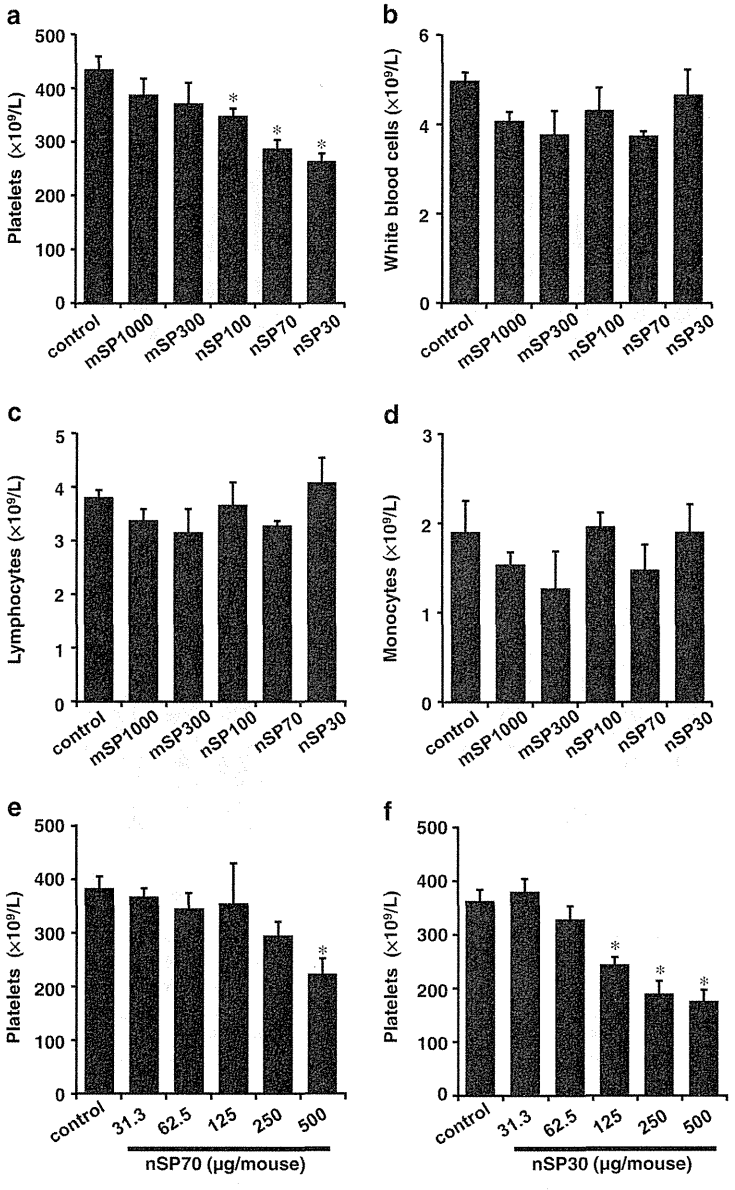

Figure 4 Hematological analysis. BALB/c mice were intranasally exposed to nSP30, nSP70, mSP300, nSP100, or mSP1000 at a concentration of 500 μg/mouse in **(a-d)**, and 31.3-500 μg/mouse in **(e,f)** for 7 days. Twenty-four hours after the final administration, **(a,e,f)** platelets, **(b)** white blood cells, **(c)** lymphocytes, and **(d)** monocytes were analyzed. Results are expressed as mean ± S.E. (n = 5). *Represents significant difference from the control ($p < 0.05$).

increase with decreasing particle size (Figure 6b,c). These results suggest that the activation of an intrinsic coagulation pathway by nanosilica particles after intranasal administration was promoted by the activation of coagulation factor XII and platelets.

Discussion

Merget *et al.* suggested that the inhalation of amorphous silica particles in the workplace could induce silicosis [22]. In addition, nanosilica particles have been explored for medical applications, such as cancer therapeutics or drug-delivery agents *via* intranasal administration [23,24]. However, there is not enough information about the biological effects of nanosilica particles after intranasal exposure for them to be used safely. In this study, we focused on intranasal exposure of nanosilica particles and determined the localization and biological effects of nanosilica particles after intranasal administration.

Warheit *et al.* and Lee *et al.* reported that the no-observable-effect level (NOEL) of colloidal silica particles

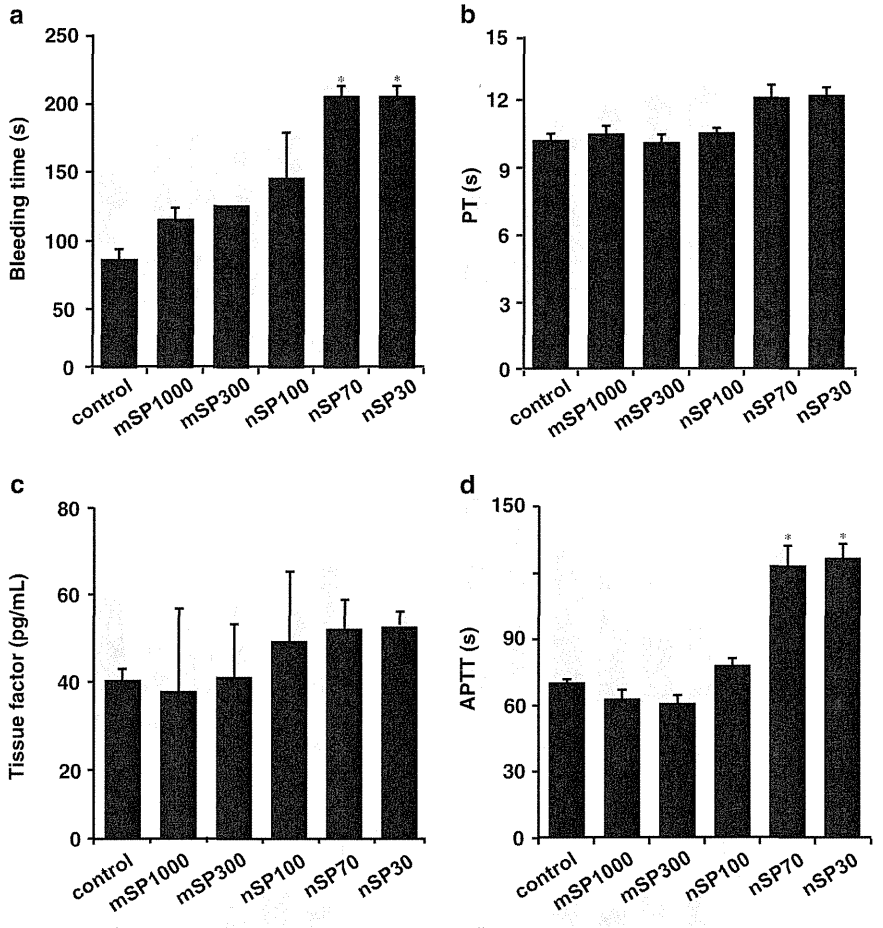

Figure 5 Examination of coagulation cascade. BALB/c mice were intranasally exposed to nSP30, nSP70, mSP300, nSP100, or mSP1000 at a concentration of 500 μg/mouse for 7 days. Twenty-four hours after the final administration, **(a)** bleeding time (evaluated by Duke's method), **(b)** prothrombin time (PT) and **(d)** activated partial thromboplastin time (APTT) were evaluated. **(c)** The level of tissue factor (TF) in plasma was determined using ELISA. PT and APTT in collected plasma were determined at 37°C in the Clotek dry-block heating system with PT and APTT reagents. Results are expressed as mean ± S.E. (n = 4–5). *Represents significant difference from the control ($p < 0.01$).

is 489 μg/lung (equivalent to an inhalation exposure of 10 mg/m^3) [25,26]. Accordingly, we designed our experiments such that mice were intranasally exposed to various sizes of silica particles at 500 μg/mouse for 7 days, a level close to the NOEL for inhalation exposure. The dose in our study is important from the viewpoint of establishing an upper threshold for the amount of NMs that can safely be administered intranasally. Although we still need to accumulate much more information about the biological effects of nanosilica particles using intranasal administration, at realistic exposure levels, we expect that our present study will contribute to the safety assessment of NMs.

We found that nSP30, nSP70, and nSP100 were located not only in the nasal cavity and lung but also in the liver (Figure 1). In our previous study, we showed that nSP70, mSP300, and mSP1000 localized in the liver after entering the bloodstream [11]. When we hypothesize how the nanosilica particles (smaller than 100 nm) enter the liver after intranasal administration, it is important to discuss how nanosilica particles enter the bloodstream through the nasal cavity or lung. We hypothesized that the nanosilica particles were absorbed through transcytosis, or uptake by microfold cells (M cells) in bronchus-associated lymphoid tissues and nasal-associated lymphoid tissues. Other reports have suggested that NMs open the tight junction, which plays an important role in maintaining the epithelial barrier [27,28]. Thus, to investigate the pathway by which nanosilica particles enter the body, we need to evaluate the effects of nanosilica particles on M cells or epithelial cell barriers *in vitro*. In this study, we examined only the nasal cavity, lung, and liver, so we cannot comment as to whether nanosilica particles are localized in other tissues. However, other groups have reported that

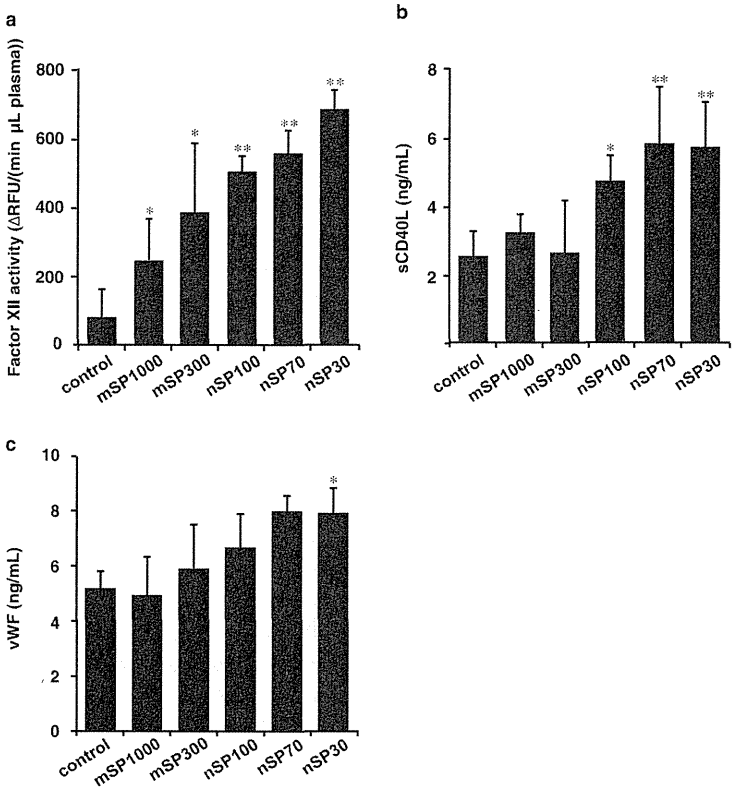

Figure 6 Examination of intrinsic cascade pathways. (a) *In vitro* changes in blood coagulation factor XII activity in human plasma by silica particles of various sizes. The initial rate of reaction of coagulation factor XII was obtained from human plasma, which was obtained from a control sample of human plasma, which did not contain any silica particles, and was measured by fluorescence intensity. Results are expressed as mean ± S.D. ($n = 5$). ** and * represent significant differences from the control (**$p < 0.01$, *$p < 0.05$). RFU: relative fluorescent unit. **(b)** The level of soluble CD40 ligand (sCD40L) and **(c)** the level of von Willebrand factor (vWF) in mouse plasma. BALB/c mice were intranasally exposed to nSP30, nSP70, mSP300, nSP100 or mSP1000 at a concentration of 500 μg/mouse for 7 days. Twenty-four hours after the final administration, the levels of sCD40L and vWF in the mouse plasma were determined using ELISA. Results are expressed as mean ± S.E. ($n = 4$–5). ** and * represent significant differences from the control (**$p < 0.01$, *$p < 0.05$).

titanium dioxide nanoparticles with a diameter of 80 nm were localized in the brain after intranasal administration [29,30]. Furthermore, Liu *et al.* showed that copper nanoparticles with a diameter of 23.5 nm enter the olfactory bulb in the brain [31]. Therefore, in our study, it is possible that nanosilica particles with diameters of 30 or 70 nm may have been localized in the brain. In this analysis, the particles detected in tissues after intranasal administration of mSP300 and mSP1000 were smaller than the average diameter of the respective administered particles (Figure 1a,b,e). We consider the possibility of degradation of mSP300 and mSP1000 in the body, because some previous *in vitro* studies have suggested that silica particles could be degraded in humans and animals after absorption [32-34]. For example, Kim *et al.* showed that approximately 50% to 80% of a sample of microsilica particles was dissolved within 36 h in a solution of phosphate-buffered saline with 10% bovine serum, which is a simulated body fluid [32]. In addition, a recent study suggested the possibility of silica particle degradation at a cellular level. Zhai *et al.* showed that hollow mesoporous nanosilica particles degraded when injected into human umbilical vein endothelial cells [33]. On the basis of these reports' findings, silica particles localized in biological bodies might be degraded within 7 days by means of interaction with biological fluid or by uptake into epithelial cells in the nasal cavity or lungs. On the other hand, because transmission electron microscopy analysis is only a qualitative method, we need to quantitatively analyze the silica particles after intranasal exposure to obtain more detailed information about their biodistribution. Inductively coupled plasma–optical emission spectrometry (ICP-OES) is reported to be a suitable means for quantitatively measuring silica. Using ICP-OES, we initially attempted to quantify the absorption of nSP30 and nSP70 in the liver after intranasal exposure for 7 days. However, we did not detect the particles in biological tissue using ICP-OES (data not shown; the detection limit of our protocol was 50 μg/g). In our study,

nanosilica particles were not localized in the liver at levels sufficient for measurement by ICP-OES. To quantitatively analyze the nanosilica particles and clarify their absorption, distribution, metabolism, and excretion mechanisms, a method with greater sensitivity must be developed.

Previously, we found that nanosilica particles could accumulate in the liver and induce severe liver damage after intravenous administration [11,15]. The level of nanosilica particles accumulated in the liver after intranasal administration would be lower than that observed after intravenous administration, and thus a nanosilica-particle-mediated increase of ALT levels or abnormal findings in pathological examination would have been reduced in the present study. We must measure the level of nanosilica particles in the liver quantitatively to confirm this speculation; overall, our present findings suggest that we need to more precisely evaluate the biological effects of intranasally administered NMs on all tissues in the body, including the liver and brain.

Intranasally administered nanosilica particles might have induced abnormal activation of the intrinsic coagulation cascade (Figures 4 and 5). To explain the decrease of platelets observed in the nanosilica-particle-treated groups, the nanosilica particles might directly activate the platelets and promote the coagulation cascade, resulting in consumption of platelets and consequently prolonged bleeding times. Other groups have shown that some NMs, such as single-walled carbon nanotubes and rutile titanium dioxide nanorods, could activate platelets and induce abnormal activation of the coagulation system [35-38]. Therefore, in our study the platelets might have been activated by the nanosilica particles and then subsequently consumed as they formed blood clots, thus decreasing the number of platelets and consequently prolonging bleeding time. Furthermore, the platelet counts in the nSP70-treated group at concentrations <250 μg/mouse and in the nSP30-treated group at concentrations <62.5 μg/mouse were equal to the count of the control group. Thus, this finding could provide useful information for setting the no-observable-adverse-effect level for intranasally administered nanosilica particles. Our present results indicate that the abnormal activation of a coagulation cascade by nanosilica particles after intranasal administration was promoted by activation of an intrinsic cascade pathway (Figure 5). However, our previous study showed that intravenously administered nSP70 could induce the release of TF, which is a known marker of activation of an extrinsic cascade pathway [15]. We speculate that the level of intranasally administered nanosilica particles in the bloodstream was lower than that of intravenously administered nanosilica particles, and thus a drastic release of TF was not detected in this study.

Contact activation of coagulation factor XII is one of the major factors of blood coagulation [39,40], and, as mentioned earlier, coagulation factor XII is activated when it comes into contact with hydrophilic activating particles (such as fully water-wettable glass) [18]. Since the number of silica particles per unit weight increases as the particle size decreases (the particle numbers of the silica particles were 3.5×10^{13}, 2.8×10^{12}, 9.5×10^{11}, 3.5×10^{10}, and 9.5×10^{8} particles/mg for nSP30, nSP70, nSP100, mSP300, and mSP1000, respectively), the number of opportunities for contact between the nanosilica particles and coagulation factor XII would have increased with decreasing particle size, thus ultimately leading to the activation of coagulation factor XII. In addition, we need to take into account not only the number of silica particles but also the surface area. The intrinsic cascade pathway involves various factors, such as factor XI and prekallikrein. Therefore, to reveal the mechanism of abnormal activation of the coagulation cascade by nanosilica particles, we need to examine the effects of nanosilica particles on other factors in intrinsic cascade pathways. Increases in the levels of sCD40L and vWF were observed in plasma from the nSP30- and nSP70-treated groups (Figure 6), meaning that nanosilica particles absorbed into the bloodstream induced activation of platelets, which are involved in the activation of coagulation pathways. Although we need to evaluate in greater detail the effects of nanosilica particles on activation or aggregation of platelets, our results and these previous reports suggest that nanosilica particles would induce platelet activation, resulting in activation of an intrinsic cascade pathway. Tavano *et al.* suggested that synthetic amorphous silica (SAS), which is similar to our silica nanoparticles, and organically modified silica (ORMOSIL) nanoparticles induce significant abnormal activation of the coagulation system *via* a different mechanism in *in vitro* studies [41]. More specifically, SAS nanoparticles activate contact coagulation (factor XII dependent) but not TF transcription in monocytes. In contrast, ORMOSIL nanoparticles induce TF-dependent coagulation more efficiently than SAS nanoparticles. The group's report indicated that the activation of an intrinsic cascade pathway is the main mechanism of amorphous silica nanoparticle–mediated procoagulant activity, thus supporting our study's conclusions and reiterating the importance of examining the effects of silica nanoparticles on intrinsic coagulation.

In summary, we revealed that intranasally administered nanosilica particles have the potential to induce abnormal activation of a coagulation cascade in mice. Recently, nanosilica particles have been used in food additives and cosmetics, and thus opportunities for such particles to be inhaled by workers during manufacturing are increasing [4,42]. Furthermore, nanosilica particles are being explored as cancer therapy and drug-delivery agents, and might be administered intranasally in such

applications as well [23,24]. Therefore, the localization and biological effects of intranasally administered nanosilica particles must be elucidated. We expect that further studies of the relationship between localization and biological effects will provide useful information for the development of safer, effective NMs.

Conclusions

We have shown that nanosilica particles with diameters of 30, 70, and 100 nm intranasally administered to mice were absorbed into the bloodstream and distributed into certain organs, such as the liver. The obtained results suggest that the activation of an intrinsic cascade pathway induced by nanosilica particles with diameters of 30 and 70 nm, both of which activated coagulation factor XII and platelets, could result in abnormal activation of the coagulation system. We expect that the findings of this study will contribute to the ongoing development of NMs that are safe for use in humans and animals.

Methods

Silica particles

Amorphous nanosilica particles with diameters of 30, 70, and 100 nm, as well as microscale silica particles with diameters of 300 and 1000 nm (Micromod Partikeltechnologie, Rostock/Warnemünde, Germany, designated nSP30, nSP70, nSP100, mSP300, and mSP1000, respectively) were used in this study. The particle numbers of the silica particles were 3.5×10^{13}, 2.8×10^{12}, 9.5×10^{11}, 3.5×10^{10}, and 9.5×10^{8} particles/mg for nSP30, nSP70, nSP100, mSP300, and mSP1000, respectively. Each type of silica particles was sonicated for 5 min and vortexed for 1 min before use.

Animals

BALB/c mice (female, 6–8 weeks) were purchased from Japan SLC, Inc. (Shizuoka, Japan). Mice were housed in a ventilated animal room maintained at 20 ± 2°C with a 12-h light/12-h dark cycle. Mice had free access to water and alfalfa-free forage (FR-2, Funabashi Farm, Funabashi, Japan). All of the animal experimental procedures in this study were performed in accordance with the National Institute of Biomedical Innovation and Osaka University Guidelines for the Welfare of Animals.

Transmission electron microscopy analysis

Five BALB/c mice were intranasally exposed to a 20 μL aliquot (10 μL per nostril) of nSP30, nSP70, nSP100, mSP300, or mSP1000 at a concentration of 500 μg/mouse for 7 days. Twenty-four hours after the final intranasal administration, the nasal cavity, lung, and liver from two mice were excised and fixed in 2.5% glutaraldehyde for 2 h. Then, small pieces of tissue sample were washed with phosphate buffer 3 times and postfixed in sodium cacodylate-buffered 1.5% osmium tetroxide for 60 min at 4°C, block-stained in 0.5% uranyl acetate, dehydrated by dipping each sample through a series of ethanol solutions containing increasing concentration of ethanol, and embedded in Epon resin (TAAB). Ultrathin sections were stained with uranyl acetate and lead citrate. The stained samples were subsequently observed under an electron microscope (H-7650, Hitachi, Tokyo, Japan).

Histopathological examination

Twenty-four hours after the final intranasal administration of each type of silica particles, the nasal cavity, lung, and liver from three mice were excised and fixed immediately in 4% paraformaldehyde. These tissues were embedded in paraffin blocks and then sliced, and the slices were placed on glass slides. After hematoxylin–eosin staining, the slides were observed, and cell aggregation in the nasal cavity, microglial aggregation in the brain, and cell aggregation and rarefaction in the liver were classified into one of five grades (0: none, 1: very slight, 2: mild, 3: moderate, 4: advanced).

Blood biomarker assay

Twenty-four hours after the final intranasal administration of each type of silica particles, blood samples were collected from the heart using plastic syringes (Terumo, Tokyo, Japan) containing 5 IU/mL heparin sodium. Plasma was harvested by centrifuging the blood at 1750 × *g* for 15 min. The levels of ALT, ALB and BUN were determined in the plasma using a biochemical autoanalyzer (Fuji dri-Chem 7000, Fujifilm, Tokyo, Japan).

Hematology analysis

Twenty-four hours after the final intranasal administration of each type of amorphous silica particles, blood samples were collected from the heart using plastic syringes (Terumo) containing 0.1 mM EDTA. Whole blood samples were analyzed with a VetScan HMII Hematology System (Abaxis, Sunnyvale, CA, USA) to determine the number of white blood cells, lymphocytes, monocytes, and platelets.

Measurement of bleeding time and coagulation tests

Twenty-four hours after the final intranasal administration of each type of silica particles, the bleeding time for each mouse was measured by Duke's method [43]. Briefly, an ear of each mouse was cut with a knife, and the blood generated at the site of the cut was absorbed with filter paper every 30 seconds until bleeding ceased. To examine the coagulation tests in each mouse, a blood sample was collected from the heart of each mouse subjected to bleeding-time tests using plastic syringes (Terumo) containing 1:9 (v/v) of 3.8% sodium citrate. Plasma was harvested by

centrifuging the blood at 1750 × *g* for 15 min. APTT and PT levels were determined at 37°C in a Clotek dry-block bath system (Hyland Division, Travenol Laboratories, Inc. Costa Mesa, CA, USA) with APTT and PT reagents (Sysmex, Kobe, Japan), respectively.

In vitro activation tests of coagulation factor XII

One hundred microliters of human health plasma (Scipac, Kent, UK) and 100 μL of various sized silica particles (3.13 mg/mL) were mixed for 1 min at room temperature with an enzyme reaction solution (50 mM Tris–HCl, 0.15 M NaCl, 1 mM $CaCl_2$ and 0.1 mg/mL bovine serum albumin, pH 8.0) containing 2 mM *t*-butyloxycarbonyl-L-glutaminyl-glycyl-L-arginine-4-methyl-courmaryl-7-amide (Peptide Institute, Inc. Ibaraki, Japan) in dimethyl sulfoxide. The initial rate of reaction was calculated by measuring the fluorescence intensity (380 nm excitation, 440 nm emission) every 5 min. The initial rate is given by Initial rate = (relative fluorescent unit of each measurement time – blank) / measurement time.

Detection of TF, sCD40L, and vWF levels in plasma

TF, sCD40L, and vWF levels in plasma were determined using enzyme-linked immunosorbent assay (ELISA) kits (TF: Mouse Tissue Factor ELISA kit (Cusabio, Newark, DE, USA); sCD40L: Mouse sCD40L ELISA (eBioscience, San Diego, CA, USA); vWF: Mouse von Willebrand Factor ELISA kit (Cusabio, Newark, DE, USA)).

Statistical analysis

Differences among each group were compared by using Williams's or Dunnett's method after analysis of variance (ANOVA).

Competing interests

The authors declare that they have no competing interests.

Authors' contributions

TY and YY designed the study. TY, ST, TH, MU, and KI performed the experiments. TY and YY collected and analyzed the data. TY and YY wrote the manuscript. KN, YA, HK, ST, HN, KH, and TY provided technical support and conceptual advice. YT supervised the project. All authors discussed the results and commented on the manuscript. All authors read and approved the final manuscript.

Acknowledgements

This study was supported, in part, by Grants-in-Aid for Scientific Research from the Ministry of Education, Culture, Sports, Science and Technology of Japan (MEXT) and from the Japan Society for the Promotion of Science (JSPS); and by the Knowledge Cluster Initiative (MEXT); by Health Labour Sciences Research Grants from the Ministry of Health, Labour and Welfare of Japan (MHLW); by a Global Environment Research Fund from the Ministry of the Environment; by Food Safety Commission (Cabinet Office); by The Cosmetology Research Foundation; by The Smoking Research Foundation; by The Research Foundation for Pharmaceutical Sciences; and by The Takeda Science Foundation.

Author details

[1]Laboratory of Toxicology and Safety Science, Graduate School of Pharmaceutical Sciences, Osaka University, 1-6 Yamadaoka, Suita, Osaka 565-0871, Japan. [2]Laboratory of Biopharmaceutical Research, National Institute of Biomedical Innovation, 7-6-8 Saitoasagi, Ibaraki, Osaka 567-0085, Japan. [3]Cancer Biology Research Center, Sanford Research/USD, 2301 E. 60th Street N, Sioux Falls SD 57104, USA. [4]The Center for Advanced Medical Engineering and Informatics, Osaka University, 1-6 Yamadaoka, Suita, Osaka 565-0871, Japan. [5]Division of Foods, National Institute of Health Sciences, 1-18-1, Kamiyoga, Setagaya-ku, Tokyo 158-8501, Japan.

Received: 14 February 2013 Accepted: 14 August 2013
Published: 20 August 2013

References

1. Sozer N, Kokini JL: **Nanotechnology and its applications in the food sector.** *Trends Biotechnol* 2009, **27**:82–89.
2. McNeil SE: **Unique benefits of nanotechnology to drug delivery and diagnostics.** *Methods Mol Biol* 2011, **697**:3–8.
3. Sonkaria S, Ahn SH, Khare V: **Nanotechnology and its impact on food and nutrition: a review.** *Recent Pat Food Nutr Agric* 2012, **4**:8–18.
4. Knopp D, Tang D, Niessner R: **Review: bioanalytical applications of biomolecule-functionalized nanometer-sized doped silica particles.** *Anal Chim Acta* 2009, **647**:14–30.
5. Maynard AD, Aitken RJ, Butz T, Colvin V, Donaldson K, Oberdorster G, Philbert MA, Ryan J, Seaton A, Stone V, *et al*: **Safe handling of nanotechnology.** *Nature* 2006, **444**:267–269.
6. Kuhlbusch TA, Asbach C, Fissan H, Gohler D, Stintz M: **Nanoparticle exposure at nanotechnology workplaces: a review.** *Part Fibre Toxicol* 2011, **8**:22.
7. Donaldson K, Poland CA: **Inhaled nanoparticles and lung cancer - what we can learn from conventional particle toxicology.** *Swiss Med Wkly* 2012, **142**:w13547.
8. Poland CA, Duffin R, Kinloch I, Maynard A, Wallace WA, Seaton A, Stone V, Brown S, Macnee W, Donaldson K: **Carbon nanotubes introduced into the abdominal cavity of mice show asbestos-like pathogenicity in a pilot study.** *Nat Nanotechnol* 2008, **3**:423–428.
9. Hougaard KS, Jackson P, Jensen KA, Sloth JJ, Loschner K, Larsen EH, Birkedal RK, Vibenholt A, Boisen AM, Wallin H, *et al*: **Effects of prenatal exposure to surface-coated nanosized titanium dioxide (UV-Titan): a study in mice.** *Part Fibre Toxicol* 2010, **7**:16.
10. Morishige T, Yoshioka Y, Tanabe A, Yao X, Tsunoda S, Tsutsumi Y, Mukai Y, Okada N, Nakagawa S: **Titanium dioxide induces different levels of IL-1beta production dependent on its particle characteristics through caspase-1 activation mediated by reactive oxygen species and cathepsin B.** *Biochem Biophys Res Commun* 2010, **392**:160–165.
11. Nabeshi H, Yoshikawa T, Matsuyama K, Nakazato Y, Matsuo K, Arimori A, Isobe M, Tochigi S, Kondoh S, Hirai T, *et al*: **Systemic distribution, nuclear entry and cytotoxicity of amorphous nanosilica following topical application.** *Biomaterials* 2011, **32**:2713–2724.
12. Yamashita K, Yoshioka Y, Higashisaka K, Mimura K, Morishita Y, Nozaki M, Yoshida T, Ogura T, Nabeshi H, Nagano K, *et al*: **Silica and titanium dioxide nanoparticles cause pregnancy complications in mice.** *Nat Nanotechnol* 2011, **6**:321–328.
13. Yoshida T, Yoshioka Y, Fujimura M, Yamashita K, Higashisaka K, Morishita Y, Kayamuro H, Nabeshi H, Nagano K, Abe Y, *et al*: **Promotion of allergic immune responses by intranasally-administrated nanosilica particles in mice.** *Nanoscale Res Lett* 2011, **6**:195.
14. Hirai T, Yoshikawa T, Nabeshi H, Yoshida T, Tochigi S, Ichihashi K, Uji M, Akase T, Nagano K, Abe Y, *et al*: **Amorphous silica nanoparticles size-dependently aggravate atopic dermatitis-like skin lesions following an intradermal injection.** *Part Fibre Toxicol* 2012, **9**:3.
15. Nabeshi H, Yoshikawa T, Matsuyama K, Nakazato Y, Arimori A, Isobe M, Tochigi S, Kondoh S, Hirai T, Akase T, *et al*: **Amorphous nanosilicas induce consumptive coagulopathy after systemic exposure.** *Nanotechnology* 2012, **23**:045101.
16. Morishige T, Yoshioka Y, Inakura H, Tanabe A, Narimatsu S, Yao X, Monobe Y, Imazawa T, Tsunoda S, Tsutsumi Y, *et al*: **Suppression of nanosilica particle-induced inflammation by surface modification of the particles.** *Arch Toxicol* 2012, **86**:1297–1307.
17. Norris LA: **Blood coagulation.** *Best Pract Res Clin Obstet Gynaecol* 2003, **17**:369–383.
18. Zhuo R, Miller R, Bussard KM, Siedlecki CA, Vogler EA: **Procoagulant stimulus processing by the intrinsic pathway of blood plasma coagulation.** *Biomaterials* 2005, **26**:2965–2973.

19. Muller F, Renne T: **Platelet polyphosphates: the nexus of primary and secondary hemostasis.** *Scand J Clin Lab Invest* 2011, **71**:82–86.
20. Blann AD: **Plasma von Willebrand factor, thrombosis, and the endothelium: the first 30 years.** *Thromb Haemost* 2006, **95**:49–55.
21. Pamukcu B, Lip GY, Snezhitskiy V, Shantsila E: **The CD40-CD40L system in cardiovascular disease.** *Ann Med* 2011, **43**:331–340.
22. Merget R, Bauer T, Kupper HU, Philippou S, Bauer HD, Breitstadt R, Bruening T: **Health hazards due to the inhalation of amorphous silica.** *Arch Toxicol* 2002, **75**:625–634.
23. Moghimi SM, Hunter AC, Murray JC: **Nanomedicine: current status and future prospects.** *FASEB J* 2005, **19**:311–330.
24. Slowing II, Vivero-Escoto JL, Wu CW, Lin VS: **Mesoporous silica nanoparticles as controlled release drug delivery and gene transfection carriers.** *Adv Drug Deliv Rev* 2008, **60**:1278–1288.
25. Warheit DB, Carakostas MC, Kelly DP, Hartsky MA: **Four-week inhalation toxicity study with Ludox colloidal silica in rats: pulmonary cellular responses.** *Fundam Appl Toxicol* 1991, **16**:590–601.
26. Lee KP, Kelly DP: **The pulmonary response and clearance of Ludox colloidal silica after a 4-week inhalation exposure in rats.** *Fundam Appl Toxicol* 1992, **19**:399–410.
27. Sonaje K, Lin KJ, Tseng MT, Wey SP, Su FY, Chuang EY, Hsu CW, Chen CT, Sung HW: **Effects of chitosan-nanoparticle-mediated tight junction opening on the oral absorption of endotoxins.** *Biomaterials* 2011, **32**:8712–8721.
28. Vllasaliu D, Exposito-Harris R, Heras A, Casettari L, Garnett M, Illum L, Stolnik S: **Tight junction modulation by chitosan nanoparticles: comparison with chitosan solution.** *Int J Pharm* 2010, **400**:183–193.
29. Wang J, Chen C, Liu Y, Jiao F, Li W, Lao F, Li Y, Li B, Ge C, Zhou G, *et al*: **Potential neurological lesion after nasal instillation of TiO(2) nanoparticles in the anatase and rutile crystal phases.** *Toxicol Lett* 2008, **183**:72–80.
30. Wang J, Liu Y, Jiao F, Lao F, Li W, Gu Y, Li Y, Ge C, Zhou G, Li B, *et al*: **Time-dependent translocation and potential impairment on central nervous system by intranasally instilled TiO(2) nanoparticles.** *Toxicology* 2008, **254**:82–90.
31. Liu Y, Gao Y, Zhang L, Wang T, Wang J, Jiao F, Li W, Liu Y, Li Y, Li B, *et al*: **Potential health impact on mice after nasal instillation of nano-sized copper particles and their translocation in mice.** *J Nanosci Nanotechnol* 2009, **9**:6335–6343.
32. Kim SF, Daniel JW, Francois LP, Anwen MKH, Hui QL, John VH, Barbé CJ: **Biodegradability of sol–gel silica microparticles for drug delivery.** *Journal of Sol-gel Science and Technology* 2009, **49**:12–18.
33. Zhai W, He C, Wu L, Zhou Y, Chen H, Chang J, Zhang H: **Degradation of hollow mesoporous silica nanoparticles in human umbilical vein endothelial cells.** *J Biomed Mater Res B Appl Biomater* 2012, **100**:1397–1403.
34. He Q, Shi J, Zhu M, Chen Y, Chen F: **The three-stage *in vitro* degradation behavior of mesoporous silica in simulated body fluid.** *Microporous and Mesoporous Materials* 2010, **131**:314–320.
35. Bihari P, Holzer M, Praetner M, Fent J, Lerchenberger M, Reichel CA, Rehberg M, Lakatos S, Krombach F: **Single-walled carbon nanotubes activate platelets and accelerate thrombus formation in the microcirculation.** *Toxicology* 2010, **269**:148–154.
36. Burke AR, Singh RN, Carroll DL, Owen JD, Kock ND, D'Agostino R Jr, Torti FM, Torti SV: **Determinants of the thrombogenic potential of multiwalled carbon nanotubes.** *Biomaterials* 2011, **32**:5970–5978.
37. Meng J, Cheng X, Liu J, Zhang W, Li X, Kong H, Xu H: **Effects of long and short carboxylated or aminated multiwalled carbon nanotubes on blood coagulation.** *PLoS One* 2012, **7**:e38995.
38. Nemmar A, Melghit K, Ali BH: **The acute proinflammatory and prothrombotic effects of pulmonary exposure to rutile TiO2 nanorods in rats.** *Exp Biol Med (Maywood)* 2008, **233**:610–619.
39. Colman RW: **Surface-mediated defense reactions. The plasma contact activation system.** *J Clin Invest* 1984, **73**:1249–1253.
40. Colman RW, Schmaier AH: **Contact system: a vascular biology modulator with anticoagulant, profibrinolytic, antiadhesive, and proinflammatory attributes.** *Blood* 1997, **90**:3819–3843.
41. Tavano R, Segat D, Reddi E, Kos J, Rojnik M, Kocbek P, Iratni S, Scheglmann D, Colucci M, Echevarria IM, Selvestrel F, Mancin F, Papini E: **Procoagulant properties of bare and highly PEGylated vinyl-modified silica nanoparticles.** *Nanomedicine (Lond)* 2010, **5**:881–896.
42. Barik TK, Sahu B, Swain V: **Nanosilica-from medicine to pest control.** *Parasitol Res* 2008, **103**:253–258.
43. Angelkort B, Zilkens KW, Wenzel E: **Bleeding time (Duke) as a clinical function test of the primary phase of hemostasis.** *Med Welt* 1976, **27**:2302–2304.

doi:10.1186/1743-8977-10-41
Cite this article as: Yoshida *et al.*: Intranasal exposure to amorphous nanosilica particles could activate intrinsic coagulation cascade and platelets in mice. *Particle and Fibre Toxicology* 2013 **10**:41.

Nanotechnology **24** (2013) 405102 (7pp) doi:10.1088/0957-4484/24/40/405102

Liver-specific microRNAs as biomarkers of nanomaterial-induced liver damage

Takashi Nagano[1,6], Kazuma Higashisaka[1,6], Akiyoshi Kunieda[1], Yuki Iwahara[1], Kota Tanaka[1], Kazuya Nagano[2], Yasuhiro Abe[3], Haruhiko Kamada[2,4], Shin-ichi Tsunoda[2,4], Hiromi Nabeshi[5], Tomoaki Yoshikawa[1], Yasuo Yoshioka[1,7] and Yasuo Tsutsumi[1,2,4,7]

[1] Laboratory of Toxicology and Safety Science, Graduate School of Pharmaceutical Sciences, Osaka University, 1-6 Yamadaoka, Suita, Osaka 565-0871, Japan
[2] Laboratory of Biopharmaceutical Research, National Institute of Biomedical Innovation, 7-6-8, Saito-Asagi, Ibaraki, Osaka 567-0085, Japan
[3] Cancer Biology Research Center, Sanford Research/USD, Sioux Falls, SD, USA
[4] The Center for Advanced Medical Engineering and Informatics, Osaka University, 1-6, Yamadaoka, Suita, Osaka 565-0871, Japan
[5] Division of Foods, National Institute of Health Sciences, Tokyo, Japan

E-mail: yasuo@phs.osaka-u.ac.jp and ytsutsumi@phs.osaka-u.ac.jp

Received 9 May 2013, in final form 23 August 2013
Published 12 September 2013
Online at stacks.iop.org/Nano/24/405102

Abstract
Although nanomaterials are being used in various fields, their safety is not yet sufficiently understood. We have been attempting to establish a nanomaterials safety-assessment system by using biomarkers to predict nanomaterial-induced adverse biological effects. Here, we focused on microRNAs (miRNAs) because of their tissue-specific expression and high degree of stability in the blood. We previously showed that high intravenous doses of silica nanoparticles of 70 nm diameter (nSP70) induced liver damage in mice. In this study, we compared the effectiveness of serum levels of liver-specific or -enriched miRNAs (miR-122, miR-192, and miR-194) with that of conventional hepatic biomarkers (alanine aminotransferase (ALT) and aspartate aminotransferase (AST)) as biomarkers for nSP70. After mice had been treated with nSP70, their serum miRNAs levels were measured by using quantitative RT-PCR. Serum levels of miR-122 in nSP70-treated mice were the highest among the three miRNAs. The sensitivity of miR-122 for liver damage was at least as good as those of ALT and AST. Like ALT and AST, miR-122 may be a useful biomarker of nSP70. We believe that these findings will help in the establishment of a nanomaterials safety-assessment system.

1. Introduction

Nanomaterials are defined as substances that have at least one dimension less than 100 nm long. They are now widely used in cosmetics, foods, and medicines because they possess innovative functions such as high electrical conductivity, tensile strength, and tissue permeability [1, 2]. However, with the development of nanomaterials has come concern that, unlike the case with microsized materials, their unique characteristics may induce unexpected biological responses [3–5]. For example, recent reports have shown that carbon nanotubes can induce mesothelioma-like lesions in mice, similar to those induced by asbestos [6]. In addition, our group has shown that silica nanoparticles with a diameter of 70 nm (nSP70) can induce severe liver damage and pregnancy complications in mice, and reactive oxygen species (ROS) generation and DNA damage *in vitro*, whereas microsized silica particles do not have these effects [7–10]. Nevertheless, because nanomaterials have the potential to improve our quality of life, it is important that we develop and promote the use of safe forms. Furthermore, the development of

[6] These authors contributed equally to the work.
[7] Address for correspondence: Laboratory of Toxicology and Safety Science, Graduate School of Pharmaceutical Sciences, Osaka University, 1-6 Yamadaoka, Suita, Osaka 565-0871, Japan.

biomarkers of the biological effects of nanomaterials would be invaluable for establishing a nanomaterials safety-assessment system and strategies for the development, production, and use of safe forms of nanomaterials. We have already explored biomarkers, with a focus on proteins, and have shown that acute-phase proteins such as haptoglobin, serum amyloid A, and C-reactive protein could be useful biomarkers of the biological effects of silica or platinum nanoparticles [11–13]. However, the use of proteins alone is not sufficient for predicting the adverse biological effects of nanomaterials, as we need to evaluate biomarkers consisting of other biological molecules.

microRNAs (miRNAs) are highly conserved and small (18- to 25-nucleotide) RNAs that play pivotal roles in gene expression—specifically at the post-transcriptional level—in plants and animals. In humans, miRNAs are involved in the regulation of development, cell differentiation, proliferation, and apoptosis [14, 15], because they regulate as many as one-third of all messenger RNAs (mRNAs) [16, 17]. Furthermore, recent reports have demonstrated that miRNAs would serve as useful biomarkers for the non-invasive, tissue-specific evaluation of diseases and drug-induced tissue damage [18, 19]. This is because they show tissue-specific expression [20, 21] and exist in a stable form in the blood, saliva, and urine [22–24].

From this perspective, we focused on miRNAs as biomarkers for predicting the biological effects of nanomaterials. Although there have been some analyses of the changes in miRNA expression following exposure to nanomaterials [25, 26], there have been very few attempts to use miRNAs as biomarkers of nanomaterials. We therefore need to collect systematic information on miRNAs as biomarkers so as to predict nanomaterials-induced biological effects and thus establish a nanomaterials safety-assessment system.

In this study, as a first trial, we attempted to investigate whether liver-specific or -enriched miRNAs (miR-122, miR-192, and miR-194) could be used as reliable biomarkers for liver damage induced by nSP70.

2. Materials and methods

2.1. Materials

Silica particles were purchased from micromod Partikeltechnologie (Rostock/Warnemünde, Germany). Silica particles with diameters of 70, 300, and 1000 nm (nSP70, nSP300, and mSP1000, respectively) were used. In addition, we used nSP70 modified with surface functional groups-a carboxyl group (nSP70-C) or an amino group (nSP70-N). The particles were sonicated for 5 min and then vortexed for 1 min before use. Lipopolysaccharide (LPS) and D-galactosamine hydrochloride (D-GalN) were purchased from Sigma-Aldrich (Tokyo, Japan).

2.2. Animals

Female BALB/c mice were purchased from Nippon SLC, Inc. (Shizuoka, Japan) and used at 6–7 weeks of age. All of the animal experimental procedures were performed in accordance with the Osaka University and National Institute of Biomedical Innovation guidelines for the welfare of animals.

2.3. Blood sample collection

BALB/c mice ($n = 5$ or 6 per group) were treated in various experiments with nSP70 at 10, 20, or 40 mg kg^{-1} or with nSP70-C, nSP70-N, nSP300, or mSP1000 at 40 mg kg^{-1}, via injection into the tail vein. As positive control of induction of liver damage, BALB/c mice ($n = 5$ or 6 per group) were intraperitoneally treated with LPS at 10 μg kg^{-1} and D-GalN at 700 mg kg^{-1}. Blood samples were collected at varying times (4, 8, 24, or 72 h after treatment) in several experiments. Sera were harvested by blood centrifugation at 8000*g* for 15 min.

2.4. Biochemical analysis

Serum levels of alanine aminotransferase (ALT) and aspartate aminotransferase (AST) were measured with a DRI-CHEM 7000 biochemical analyzer (Fujifilm Corp., Tokyo, Japan).

2.5. Isolation of total RNA from serum

We extracted total RNA, including small RNA, from serum samples by using a miRNeasy Mini Kit (QIAGEN, Tokyo, Japan) in accordance with the manufacturer's instructions. In brief, 250 μl of QIAzol lysis reagent was added to 50 μl of serum. After the addition of 50 μl of chloroform, the samples were mixed completely and centrifuged. Then, 100 μl of supernatant was transferred to a new tube and mixed with 150 μl of 100% ethanol. The sample was then applied directly to a RNeasy Mini spin column (QIAGEN) and the combined RNA to column was cleaned with wash buffers to remove impurities. Total RNA was eluted in 30 μl of RNase-free water.

2.6. Real-time quantitative reverse-transcription PCR (qRT-PCR)

Serum levels of miR-122, miR-192, and miR-194 were measured by using TaqMan RT-PCR. Each miRNA in 5 μl of purified total RNA was reverse transcribed with a miRNA-specific stem-loop reverse transcriptase primer (Life Technologies, Tokyo, Japan). TaqMan RT-PCR was performed on a StepOne Plus real-time PCR system (Life Technologies, Tokyo, Japan). Generally, typical internal controls for miRNA expression, such as U6 RNA and 5S rRNA, are degraded in serum samples [27]. Therefore, we equalized all of the conditions and then normalized the levels of each miRNA by serum volume. The expression level of each miRNA is shown as a relative fold-change. Relative expression was compared between the silica-particle-treated group and the untreated group.

2.7. Statistical analyses

All results are expressed as means ± SEM differences were compared by using the Student's *t*-test or Bonferroni test after ANOVA (analysis of variance).

3. Results

3.1. Physicochemical properties of silica nanoparticles

Silica nanoparticles are common nanomaterials that are being used in cosmetics, foods, and medicines [28, 29]. Considering that further use of silica nanoparticles is expected, it is important to assess their safety. We used silica particles with diameters of 70 nm (nSP70), 300 nm (nSP300), and 1000 nm (mSP1000), as well as nSP70 with carboxyl (nSP70-C) or amino (nSP70-N) surface functional groups. In our previous study, we confirmed by transmission electron microscopy that all silica particles of the above-listed sizes and types were smooth-surfaced spheres [7–10]. We have already shown that the hydrodynamic diameters of nSP70, nSP70-C, nSP70-N, nSP300, and mSP1000 are 64.6, 69.6, 71.8, 322, and 1140 nm, respectively, and their zeta potentials (overall surface potentials) are −52.7, −76.3, −29.0, −62.1, and −67.0 mV, respectively [7–10]. The carboxyl and amino surface modifications therefore altered the surface charge of the nSP70 particles. In addition, we have already shown that the size-distribution spectrum of each set of silica particles had a single peak, and the measured hydrodynamic diameter corresponded almost precisely to the primary particle size of each set of silica particles [7–10]. These results indicated that the silica particles used in this study were well dispersed in solution.

3.2. Liver-specific or -enriched miRNAs as biomarkers of silica nanoparticles

To evaluate the usefulness of microRNAs (miRNAs) as biomarkers for nanomaterials, we focused on a model of liver damage induced by nSP70. We have previously shown that treatment of mice with high-dose nSP70 intravenously via the tail vein induced lethal toxicity and severe liver damage. Therefore, we assessed the usefulness of the liver-specific or -enriched miRNAs miR-122, miR-192, and miR-194 as biomarkers of liver damage. miR-122 and miR-192 are the two miRNAs expressed most abundantly in the human liver [30], and hepatic miR-194 is highly expressed in hepatic epithelial cells, including hepatocytes, which are parenchymal cells and account for more than 80% of liver cells [31]. Therefore, to collect systematic information on whether miRNAs have the potential to be biomarkers of nanomaterials, we selected those three major miRNAs in liver. Mice were given nSP70, nSP300, or mSP1000 via the tail vein. A dose rate of 40 mg kg^{-1} was chosen, because in the case of nSP70 this dose rate significantly increases the levels of ALT and AST [10]. As positive control, mice were intraperitoneally treated with LPS and D-GalN. At 8 h after treatment, we evaluated the serum level of each miRNA by using qRT-PCR and those of ALT and AST (i.e. the conventional hepatic biomarkers) by using biochemical analysis. The levels of miR-122 (figure 1(A)), ALT (figure 1(B)), and AST (figure 1(C)) in LPS/D-GalN-treated mice were significantly increased compared to those of vesicle-treated mice. The levels of miR-122 (figure 1(A)) and miR-192 (figure 1(D)) in nSP70-treated mice were significantly greater than those in saline-, nSP300- or mSP1000-treated mice and untreated mice. In contrast, the serum levels of miR-194 did not differ significantly among any groups (figure 1(E)). In addition, the levels of ALT (figure 1(B)) and AST (figure 1(C)) in nSP70-treated mice were significantly greater than those in saline-, nSP300- or mSP1000-treated mice and untreated mice. Thus, miR-122 and miR-192 may be useful as biomarkers for evaluating liver damage induced by nSP70. We focused on miR-122 in the following assessment, because it had the highest rate of expression among the three miRNAs.

3.3. Sensitivity and time-dependency of miR-122 expression

To more precisely assess the serum levels of miR-122 as a biomarker, we examined the sensitivity and time-dependency of miR-122 expression after treatment with nSP70. Mice were intravenously treated with nSP70 at 10, 20, or 40 mg kg^{-1}. Blood samples were collected 8 h after treatment and the levels of miR-122, ALT, and AST were measured. The serum levels of miR-122 (figure 2(A)), ALT (figure 2(B)), and AST (figure 2(C)) showed dose-dependent patterns of expression. In mice treated with 40 mg kg^{-1} nSP70 and 20 mg kg^{-1} in the case of AST, the levels of all three markers were significantly greater than in untreated or saline-treated mice. Thus, as was the case with ALT and AST, the increase in serum miR-122 levels was dependent on the dose of nSP70. Next, to assess the time-dependency of miR-122 expression, we examined the serum levels of miR-122 (figure 2(D)), ALT (figure 2(E)), and AST (figure 2(F)) at 4, 8, 24, and 72 h after intravenous injection of nSP70 at 40 mg kg^{-1}. The serum levels of miR-122 in nSP70-treated mice were significantly higher than those in saline-treated mice at every time point, as was the case with ALT and AST. These results suggested that the pattern of release of miR-122 into the blood was the same as those of ALT and AST.

3.4. miR-122 response after treatment of mice with surface-modified nSP70

Our group has previously demonstrated that modification of nSP70 with surface functional groups such as a carboxyl group (nSP70-C) or amino group (nSP70-N) can reduce the toxic effects of nSP70 (e.g., pregnancy complications in mice and ROS generation and DNA damage *in vitro*) [8, 9]. Here, we tested the use of miR-122 as a biomarker to determine whether the safety of nSP70 could be improved by adding functional groups. BALB/c mice were treated intravenously with nSP70, nSP70-C, or nSP70-N at 40 mg kg^{-1}. At 8 h after treatment, we measured the levels of miR-122 (figure 3(A)), ALT (figure 3(B)), and AST (figure 3(C)). The serum levels of miR-122 in nSP70-C- or nSP70-N-treated mice were significantly lower than that in nSP70-treated mice and were almost the same as those in untreated or saline-treated mice. The serum levels of ALT after treatment with nSP70-C or nSP70-N showed a trend similar to those of miR-122. In contrast, although the level of AST in nSP70-N-treated mice was significantly lower than that in nSP70-treated mice, the

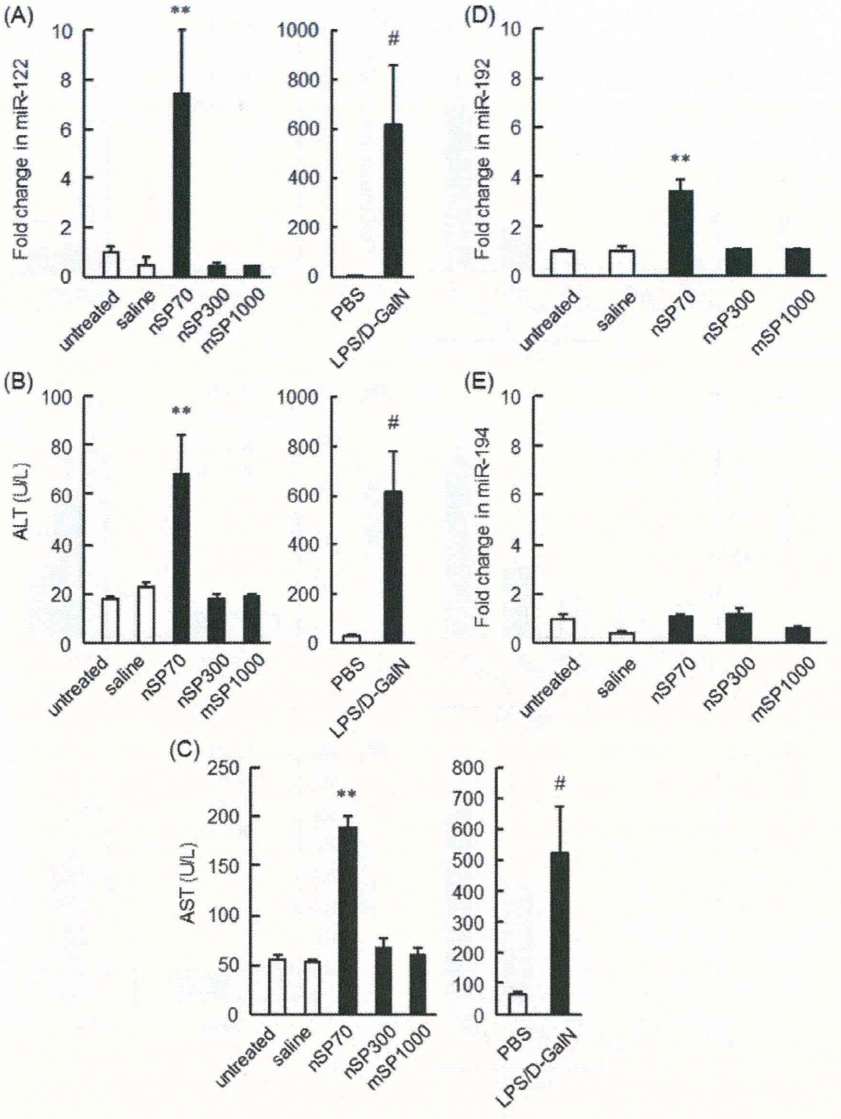

Figure 1. Usefulness of liver-specific microRNAs (miR-122, miR-192, and miR-194) as biomarkers for the development of safe silica nanoparticles. BALB/c mice were intravenously treated with nSP70, nSP300, or mSP1000 at 40 mg kg^{-1}. In addition, as positive control, mice were intraperitoneally treated with LPS and D-GalN. After 8 h, the serum levels of each microRNA, (A) miR-122, (D) miR-192, and (E) miR-194, were examined by real-time quantitative reverse-transcription PCR. Serum levels of (B) alanine aminotransferase (ALT) and (C) aspartate aminotransferase (AST) were measured by biochemical analysis. Data are presented as means ± SEM ($n = 6$; $^{**}P < 0.01$ versus value for saline-, nSP300-, mSP1000-treated group and untreated group by ANOVA; $^{\#}P < 0.05$ versus value for PBS-treated group by Student's *t*-test).

AST level in nSP70-C-treated mice was significantly greater than that in untreated or saline-treated mice. These results suggest that serum miR-122 may be useful as a biomarker for assessing improvement of the safety of nSP70 through surface modification.

4. Discussion

Our group showed previously that nSP70 can induce severe liver damage in mice [10]. Here, we examined whether liver-specific or -enriched miRNAs (miR-122, miR-192, and miR-194) were potentially useful as biomarkers of the liver damage induced by nSP70. Although miR-192 and miR-194 are thought to be involved in controlling proliferation and metastasis in liver cancer, the details of their functions are less well understood than in the case of miR-122 [31]. miR-122 is a key regulator of cholesterol and fatty-acid metabolism in the liver [32]. Therefore, it is likely that changes in the levels of miR-122 will predict not only liver damage but also the biological effects of that damage, such as abnormalities in fat metabolism. In addition, miR-122 has also been shown to be biomarkers for drug-induced liver injury in mice, rats, and human [33–35].

First, we showed that serum levels of miR-122 and miR-192 in nSP70-treated mice were elevated 8 h after treatment (figures 1(A) and (D)), as were those of ALT and AST (figures 1(B) and (C)), and that the levels of miR-122

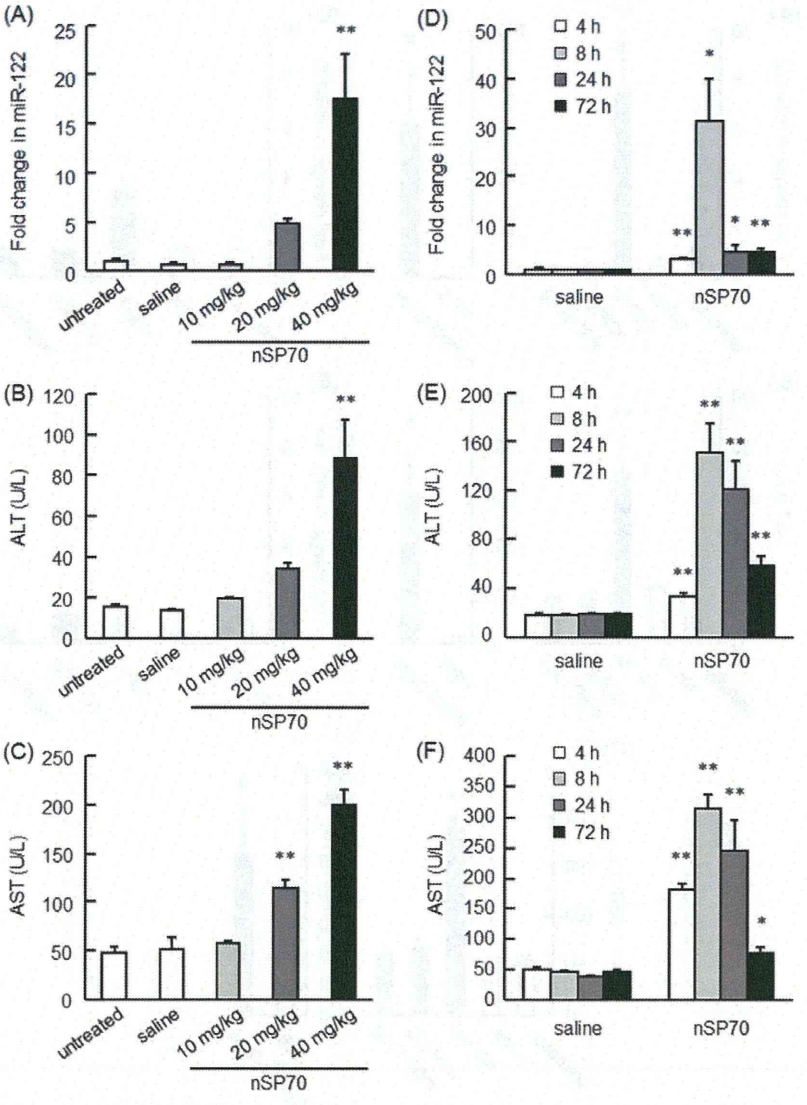

Figure 2. Serum levels of miR-122 after treatment with nSP70. BALB/c mice were intravenously treated with nSP70 at 10, 20, or 40 mg kg^{-1}. At 8 h after treatment with nSP70, the levels of (A) miR-122, (B) alanine aminotransferase (ALT), and (C) aspartate aminotransferase (AST) were analyzed. In addition, at 4, 8, 24, and 72 h after treatment with nSP70 at 40 mg kg^{-1}, the levels of (D) miR-122, (E) ALT, and (F) AST were examined. Data are presented as means ± SEM ($n = 5$ or 6; $^{*}P < 0.05$, $^{**}P < 0.01$ versus value for saline-treated group and untreated group by ANOVA).

were much higher than those of miR-192. We considered that this was because miR-122 accounts for 70% of all liver miRNA. By contrast, the serum levels of miR-194 in nSP70-treated mice did not differ significantly from those in untreated or saline-treated mice (figure 1(E)). The expression of miR-194 may change markedly with time; because we analyzed this expression only at 8 h after treatment, further time-course studies are needed before this miRNA can be discarded as a biomarker.

The serum levels of ALT and AST in mice treated with nSP70 at 40 mg kg^{-1} were beyond the physiological range, at about 4 times the values in untreated or saline-treated mice. In contrast, the serum level of miR-122 in nSP70-treated mice was about 15 times that in untreated or saline-treated mice (figures 2(A)–(C)). This suggests that miR-122 may be a more sensitive biomarker than the currently used ALT and AST in detecting liver damage induced by nSP70. In addition, as shown in figures 2(A)–(C), we evaluated the dose-dependent expression of miR-122 only at 8 h after treatment with nSP70, and we showed that the pattern of expression of miR-122 was almost the same as that of ALT and AST. In another study, injection of acetaminophen did not cause serum ALT elevation at 1 h, although obvious increases in miR-122 and miR-192 levels were already observable [36]. Therefore, evaluation at time points earlier than 8 h after nSP70 injection with lower doses could reveal the possibility that miR-122 is a more sensitive predictor of nSP70-induced liver damage than ALT and AST.

As shown in figures 2(D)–(F), the serum levels of ALT and AST in mice treated with nSP70 at 24 h showed significantly greater than those in saline-treated mice, while for miRNA-122, it dropped at 24 h to the same level as

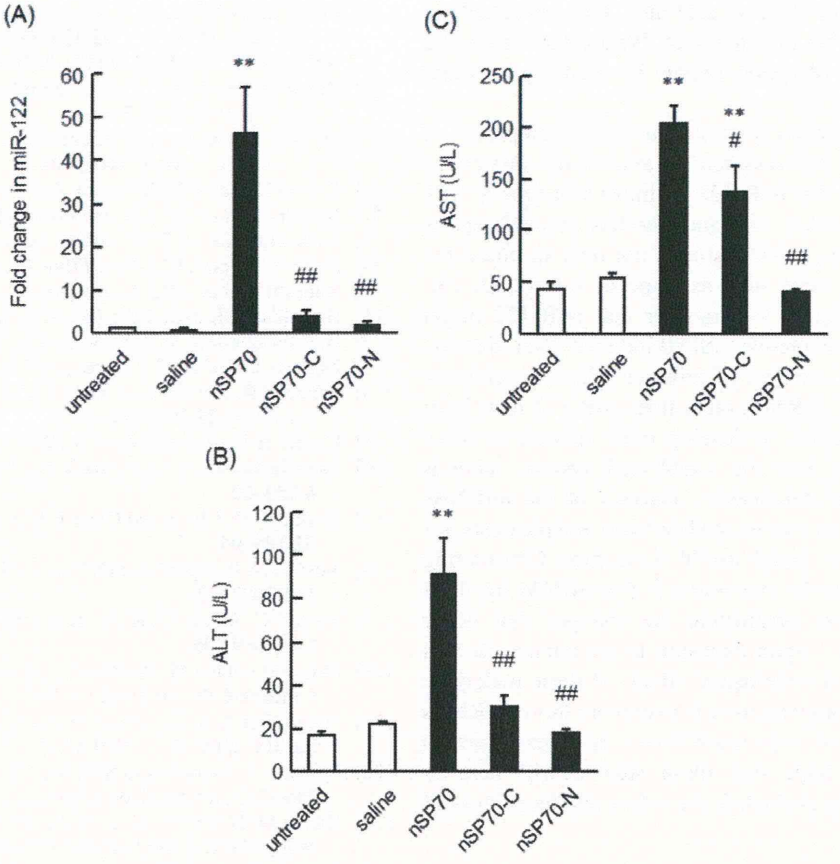

Figure 3. Responses of serum levels of miR-122 to treatment with surface-modified nSP70. BALB/c mice were intravenously treated with nSP70, nSP70-C, or nSP70-N at 40 mg kg^{-1}. Serum levels of (A) miR-122, (B) alanine aminotransferase (ALT), and (C) aspartate aminotransferase (AST) were measured 8 h after treatment. Data are presented as means ± SEM ($n = 5$ or 6; $^{**}P < 0.01$ versus value for saline-treated group and untreated group; $^{\#}P < 0.05$, $^{\#\#}P < 0.01$ versus value for nSP70-treated group by ANOVA).

72 h. In general, miRNAs are considered to be stable in the blood [37]. However, Yamaura *et al* showed that although miR-122 was stable in human plasma, it was unstable in rat plasma [38]. Therefore, although detailed information on the stability of mouse miR-122 is unavailable, it is possible that RNase action in the blood leads to a rapid decrease in miR-122 levels. Currently, there are two hypothetical pathways by which miRNAs can enter the circulation [39]. One is by direct leakage from cells, and the other is by release from cells via microvesicles. It is thought that direct secretion of miRNAs occurs in tissue damage or cell apoptosis [39]. We previously demonstrated that nSP70 administered via the tail vein was distributed mainly to the liver and induced cytotoxicity in primary hepatocytes isolated from nSP70-treated mice [7]. Taking these results together, it is conceivable that most miR-122 is leaked into the blood and degraded by RNase between 8 and 24 h after nSP70 treatment. On the other hand, the level of miR-122 in nSP70-treated mice showed significant increments compared to that of saline-treated mice over the time course of the experiment. Therefore, its change in expression over the full time course of the experiment was still useful for evaluating nSP70-induced liver damage. For these reasons, we consider that miR-122 is as useful as ALT and AST in evaluating nSP70-induced liver damage. However, because we cannot explain this in detail, we are now trying to investigate the mechanism involved.

Here, we evaluated the time course of miR-122 expression over only a short period of time after nSP70 treatment. However, considering that we are exposed to nanomaterials on a daily basis, there is a need to investigate the biological effects of long-term exposure to them. Recent reports have shown that long-term exposure to titanium dioxide nanomaterials in mice induces ROS production in the lung [40]. A nanomaterials safety-assessment system is required for the evaluation of not only acute effects but also chronic effects. Therefore, we intend to analyze nanomaterial-induced chronic biological effects by evaluating the long-term course of miRNA expression.

Although the levels of miR-122, ALT, and AST were lower in mice treated with modified nSP70 than in those treated with unmodified nSP70 (figure 3), the AST level in nSP70-C-treated mice was higher than that in untreated mice. It is possible that nSP70-C and nSP70-N is safer than nSP70, because we previously demonstrated that differences in the surface charge state or kind of functional group of nanomaterials lead to different biological effects and cell responses [41–43]. On the other hand, AST is abundant not only in the liver but also in the skeletal muscle, heart, and kidney. Taking these results together, we consider that the